Nanoscale

Highly selective encapsulation and purification of U-based C_{78}-EMFs within a supramolecular nanocapsule

Journal:	*Nanoscale*
Manuscript ID	NR-ART-09-2019-007660.R1
Article Type:	Paper
Date Submitted by the Author:	17-Oct-2019
Complete List of Authors:	Fuertes, Carles; Universitat de Girona, Institut de Química Computacional i Catàlisi (IQCC) and Departament de Química Murillo, Jesse; University of Texas at El Paso, Chemistry Soto, Marco E.; University of Texas at El Paso Morales-Martínez, Roser; Universitat Rovira i Virgili, Rodriguez-Fortea, Antonio; Universitat Rovira i Virgili, Dept. Quimica Fisica i Inorganica Poblet, Josep; Universitat Rovira i Virgili, Química Física i Inorgànica Echegoyen, Luis; University of Texas at El Paso, Department of Chemistry Ribas, Xavi; Universitat de Girona, Institut de Química Computacional i Catàlisi (IQCC) and Departament de Química

ARTICLE

Highly selective encapsulation and purification of U-based C_{78}-EMFs within a supramolecular nanocapsule

Received 00th January 20xx,
Accepted 00th January 20xx

DOI: 10.1039/x0xx00000x

Carles Fuertes-Espinosa,[a] Jesse Murillo,[b] Marco E. Soto,[b] Roser Morales-Martínez,[c] Antonio Rodríguez-Fortea,[c] Josep M. Poblet,[c] Luis Echegoyen,*[,b] and Xavi Ribas*[,a]

The ability of the tetragonal prismatic nanocapsule **1**·$(BArF)_8$ to selectively encapsulate U-based C_{78} EMFs from soot mixture is reported, showing enhanced affinity for C_{78}-based over C_{80}-based EMFs. Molecular recognition driven by the electrostatic interactions between host and guest is at the basis of the high selectivity observed for flattened C_{78}-based EMFs compared to spherical C_{80}-based EMFs. In addition, DFT analysis points towards an enhanced breathing adaptability of nanocapsule **1**·$(BArF)_8$ to C_{78}-based EMFs to further explain the selectivity observed when the host is used in the solid phase.

Introduction

Since the discovery of fullerenes in 1985, great interest has been devoted to exploit the cavity of the carbon cages for hosting guest atoms or molecules. Specifically, Endohedral Metallofullerenes (EMFs) typically feature monoatomic or diatomic metal cations of the type $X@C_{2n}$, $X_2@C_{2n}$ (X=metal, and $60 \leq 2n \leq 88$), and also metal clusters such as trimetallic nitrides (M_3N), dimetallic carbides (M_2C and M_2C_2) and metallic oxides and sulphides (M_4O_2, M_2O, M_2S) have been described, among others.[1, 2] The interest for these species are multiple: a) intrinsic nature of the interaction of the naked cation(s) with the carbon cage,[3, 4] b) the unprecedented electronic and magnetic properties of the EMF due to stabilization of otherwise non-existing clusters,[5] c) the cluster-dependent exohedral reactivity of the EMF.[6-11] However, the accumulation of practical amounts of EMF to study their spectroscopy and their reactivity is hampered by three limiting factors: 1) the synthesis of soot with significant amounts of the desired EMF, 2) the lack of selectivity during their production, and 3) tedious and time-consuming HPLC chromatographic techniques to enrich or purify the selected EMF. Even more challenging is the chromatographic separation of EMFs with the same carbon cage and differing only in the nature of the cluster.[12] Alternative non-chromatographic approaches include the "stir and filter" method (SAFA) that consists in the immobilization of empty cyclopentadienyl- and amino-functionalized silica to enrich the soot with EMFs.[13, 14] Also, the addition of Lewis acids such as $FeCl_3$, $AlCl_3$ or $TiCl_4$ allowed to separate EMFs upon precipitation, while empty fullerenes remained in solution.[15] However, these methods are commonly used as a pre-enrichment of EMFs of a given soot and HPLC chromatography is ultimately necessary. On the other hand, Echegoyen reported the electrochemical purification of Sc_3N-based EMF.[16]

In the past years, scarce examples of the encapsulation of EMFs in supramolecular hosts have been reported, i.e. $Sc_3N@C_{80}$ or $Gd@C_{82}$.[17-19] Very recently, our group has developed the purification of EMFs by selective encapsulation in supramolecular nanocapsules. Following this strategy, we have recently reported the purification and isolation of $Sc_3N@C_{80}$ (I_h–D_{5h} mixture),[20] $U_2@I_h$-C_{80} and $Sc_2CU@I_h$-C_{80} from different soots.[21] In this work, we expand the ability of the tetragonal prismatic nanocapsule **1**·$(BArF)_8$ to selectively encapsulate novel U-based C_{78} EMFs, showing enhanced affinity for C_{78}-based compared to C_{80}-based EMFs (Figure 1). The high selectivity observed is discussed based on the molecular recognition driven by the electrostatic interactions between host and guest. In addition, the breathing ability of our receptor in the solid phase to better adapt to C_{78}-based EMF is supported by DFT analysis.

Results and discussion

Previous investigations revealed that supramolecular nanocapsule **1**·$(BArF)_8$ is able to selectively recognize di-Uranium-based C_{80} EMFs, in the presence of many other empty fullerenes and EMFs.[21] The production of a new family of Uranium-based C_{78} EMFs allowed us to study the electronic and the shape complementarity of **1**·$(BArF)_8$ towards these new compounds, in comparison to the previously described selectivity for Uranium-based C_{80} EMFs. The low production yield and the complexity of the soots containing di-Uranium-based C_{78} EMFs makes their chromatographic separation extremely challenging. Aiming at the straightforward isolation of these new EMFs, crystals of **1**·$(BArF)_8$ were soaked in a toluene solution of the crude soot containing di-Uranium-based C_{78} EMFs along with many empty fullerenes and mono-Uranium EMF with different size carbon cages. Monitoring the host-guest complexation by LDI-TOF analysis of the species remaining in solution, we clearly observed the selective and quantitative uptake of di-Uranium-based

[a] QBIS-CAT group, IQCC and Dept. Química, Universitat de Girona, Campus de Montilivi, E-17003, Girona, Catalonia, Spain. E-mail: xavi.ribas@udg.edu
[b] . Department of Chemistry, University of Texas at El Paso, 500 West University Avenue, El Paso, Texas 79968, United States Email: echegoyen@utep.edu
[c] Departament de Química Física i Inorgánica, Universitat Rovira i Virgili, C/Marcel·lí Domingo 1, 43007 Tarragona, Catalonia, Spain.

Electronic Supplementary Information (ESI) available: [EMF soot preparation, experimental and computational details]. See DOI: 10.1039/x0xx00000x

C_{78} EMF species ($U_2@C_{78}$ and $U_2C@C_{78}$) after 3 hours, observing a drastic decrease of the peaks belonging to these compounds (Fig 2), attributed to the inclusion of the EMF within the cavity of solid **1**·$(BArF)_8$. Taking advantage of the encapsulation of the di-Uranium@C_{78} EMFs in crystalline material of the supramolecular nanocapsule, we isolated the solid (di-Uranium@ C_{78} EMFs)⊂**1**·$(BArF)_8$ complexes simply by filtration. Subsequently, the selectively trapped guests were easily released by washing the crystals with carbon disulfide, in analogy to our previously reported solvent-washing protocol (Fig 2, bottom).[22] LDI-TOF analysis of the released guests confirms an exceptional selectivity towards $U_2@C_{78}$ and $U_2C@C_{78}$ compared to the rest of the compounds present in the starting soot, including $U_2@C_{80}$, which is known to show very high affinity for **1**·$(BArF)_8$. Remarkably, the target compounds were not kinetically trapped in the cage cavity and could be easily recovered by exploiting the orthogonal solubility between the host and the guest.

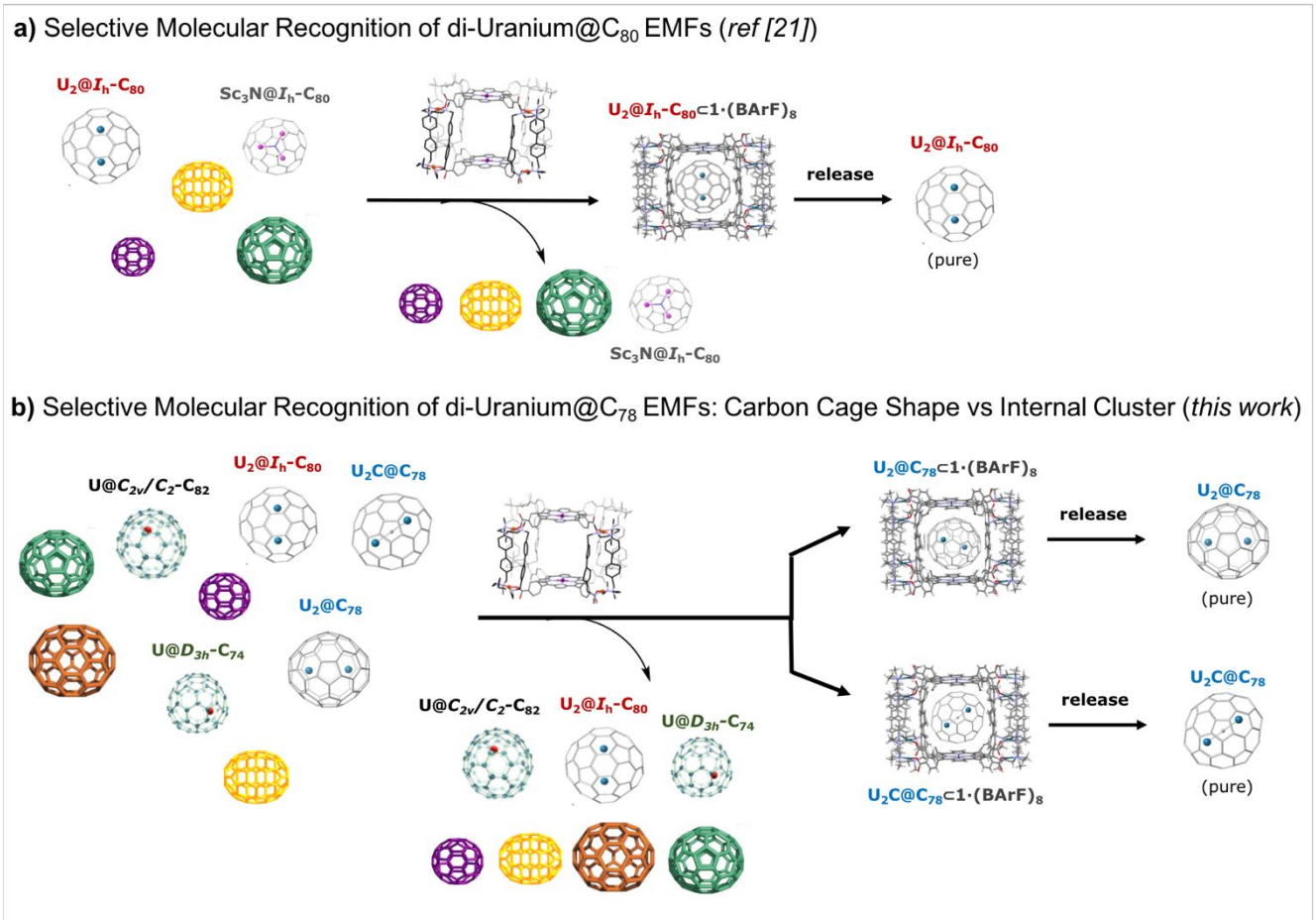

Figure 1. a) Non-chromatographic purification of U-based@C_{80} EMF by selective encapsulation in supramolecular nanocage **1a**·$(BArF)_8$. b) Highly selective encapsulation and purification of U-based@C_{78} EMFs (this work).

To better understand in the effect of the size and the shape of the guests on the specific binding observed, we then explored the molecular recognition of $U_2@C_{78}$ in the presence of a variety of U-based EMFs (U@C_{74}, U@C_{82} and $U_2@C_{80}$). Addition of crystalline **1**·$(BArF)_8$ to a toluene solution of the soot resulted in a clean and selective binding of $U_2@C_{78}$ over the rest of the EMFs (Fig. 3). The trapped guest was successfully recovered and the LDI-TOF analysis of the released EMF evidenced the unique encapsulation of $U_2@C_{78}$. The presence of the same metal cluster in $U_2@C_{78}$ and $U_2@C_{80}$, which transfer an equal number of electrons to the carbon cages, suggested that the selective molecular recognition events are governed by the size/shape relationship between the host and the guests. The crystal structures of previously reported D_{3h}–C_{78} and I_h-C_{80} EMFs showed very similar sizes of the carbon cages,[1] independently of the internal cluster hosted. Thus, the selectivity observed suggested enhanced π-interactions with the flattened regions of the ellipsoidal-shaped D_{3h}–C_{78} in comparison to the spherical I_h-C_{80} carbon cage.

Another soot containing U-based EMFs different than $U_2@C_{78}$ (with similar proportion of $U_2C@C_{78}$, $Sc_2CU@C_{80}$, U@C_{82} and $Sc_3N@C_{80}$) was the studied to evaluate the importance of the carbon cage (size and shape) or the internal cluster (electrostatics) in the observed selectivity (Fig. 4). The selective encapsulation of $U_2C@C_{78}$ was observed upon the addition of crystalline **1**·$(BArF)_8$ to the corresponding soot solution in toluene; LDI-TOF analysis revealed a

progressive decrease of the peak of $U_2C@C_{78}$ until its complete disappearance after 4.5 h (Fig. 4). LDI-TOF analysis of the released guest showed a single peak at m/z=1424.0707, confirming the purification of $U_2C@C_{78}$. Remarkably, the ability of nanocapsule **1**·$(BArF)_8$ to preferentially encapsulate C_{78} over C_{80} EMFs, was further evidenced by the encapsulation of $Sc_3N@C_{78}$ over $U_2@C_{80}$ (see Fig. S2). Therefore, the shape of the carbon cage rules over the nature of the internal cluster, with a higher affinity for C_{78}-based EMFs, irrespective of the nature of the internal cluster.

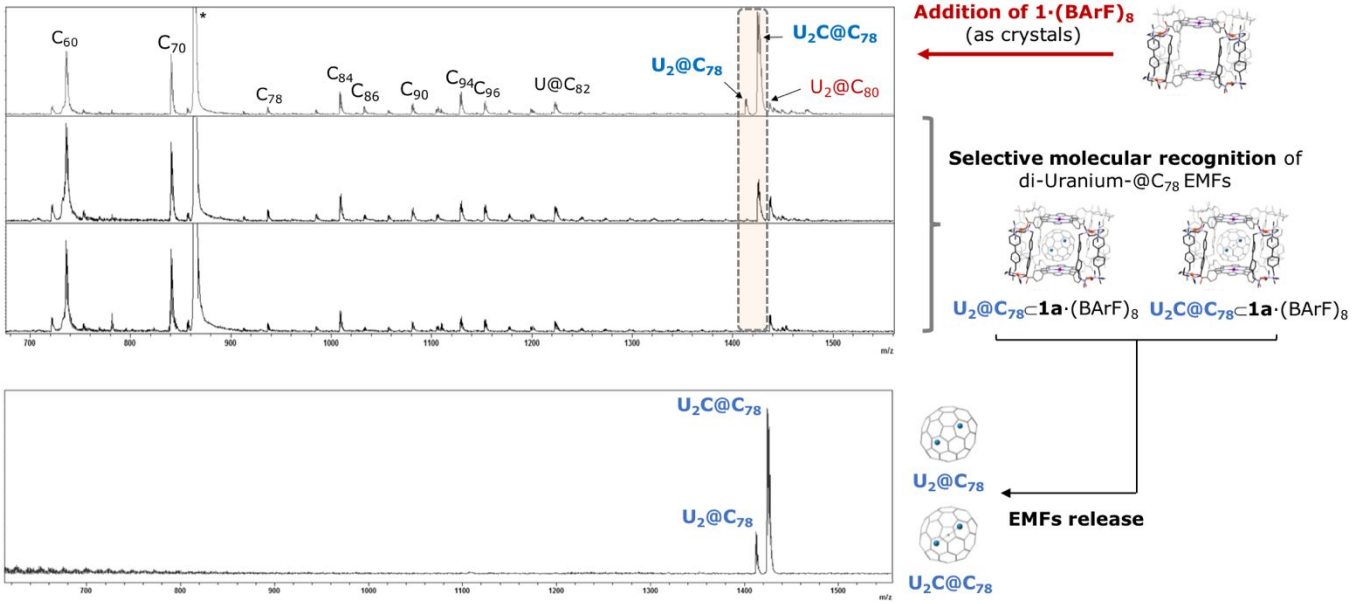

Figure 2. LDI-TOF monitoring the remaining supernatant over time during the selective encapsulation of $U_2@C_{78}$ and $U_2C@C_{78}$ within crystals of **1**·$(BArF)_8$ (top). Spectrum of released guests trapped during the molecular recognition (bottom).

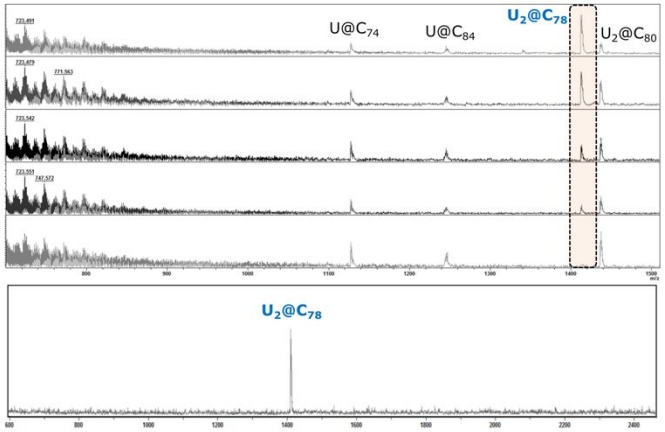

Figure 3. LDI-TOF monitoring the remaining supernatant over time during the selective molecular recognition of $U_2@C_{78}$ in a complex soot containing differently sized U-based EMFs (top). Spectrum of pure $U_2@C_{78}$ released from **1**·$(BArF)_8$ (bottom).

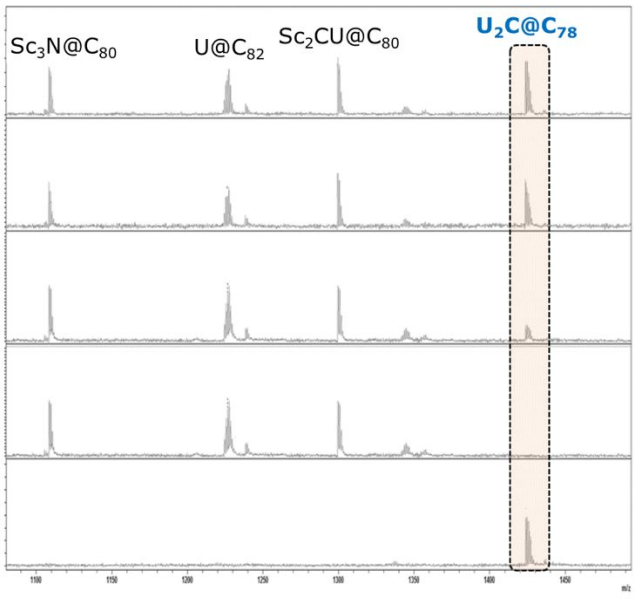

Figure 4. LDI-TOF monitoring the remaining supernatant over time during the selective molecular recognition of $U_2C@C_{78}$ in a soot containing C_{80}- and C_{82}-based EMF. Spectrum of pure $U_2C@C_{78}$ released from **1**·$(BArF)_8$ (bottom).

The presence of EMFs only differing on the nature of the internal clusters is very common in actinide-based EMFs soots, making their chromatographic separation very challenging. We previously described the important role of the electron density distribution of EMFs only differing in the internal cluster ($U_2@I_h$-C_{80} versus $Sc_2CU@I_h$-C_{80} or $Sc_3N@I_h$-C_{80}) to allow their stepwise separation within nanocapsule **1**·$(BArF)_8$.[21] We hypothesize that the differences on the cluster arrangement of $U_2@C_{78}$ and $U_2C@C_{78}$ could promote different electronic distributions that could impact the electrostatic interaction with **1**·$(BArF)_8$. Therefore, we added precise amounts of crystalline material of **1**·$(BArF)_8$ to a sample mainly containing $U_2@C_{78}$ and $U_2C@C_{78}$ (see Fig. 5). LDI-TOF monitoring showed the exclusive inclusion of $U_2@C_{78}$. LDI-TOF analysis of the released guest further confirmed the specific molecular recognition of $U_2@C_{78}$ while $U_2C@C_{78}$ remained in the starting sample solution, thus pointing towards the possible separation and purification of C_{78}-based EMF differing only in the internal cluster.

Finally, we attempted the stepwise encapsulation of $U_2@C_{78}$ and $U_2C@C_{78}$ using a complex soot, which included also $U_2@C_{80}$, mono-U-based EMF, Sc_3N-based EMF and empty fullerene cages. Monitoring the composition of the soot by LDI-TOF (Fig. 6), the peak attributed to $U_2@C_{78}$ completely disappeared (after 2 hours) upon the addition of precise amounts of **1**·$(BArF)_8$. The nanocapsule was filtered and the guest was liberated, obtaining pure $U_2@C_{78}$ as ascertained by LDI-TOF. Subsequently, additional amounts of fresh crystalline **1**·$(BArF)_8$ were added, observing a progressive selective decrease of the $U_2C@C_{78}$ peak. Liberation of the guest allowed the identification of pure $U_2C@C_{78}$.

It is worth to note that the very low concentration of the di-Uranium-based C_{78} EMFs present in the soots used makes it very complicated to spectrometrically characterize the host-guest complexes formed during the molecular recognition experiments. Despite these difficulties, the $U_2C@C_{78}\subset$**1**·$(BArF)_8$ complex was identified by ESI-MS (see Fig. S1).

The encapsulation of $Sc_3N@C_{78}$ in **1**·$(BArF)_8$ in front of $Sc_3N@C_{80}$ is thermodynamically and also kinetically preferred, as demonstrated by competition experiments shown in Figures S3 and S4.

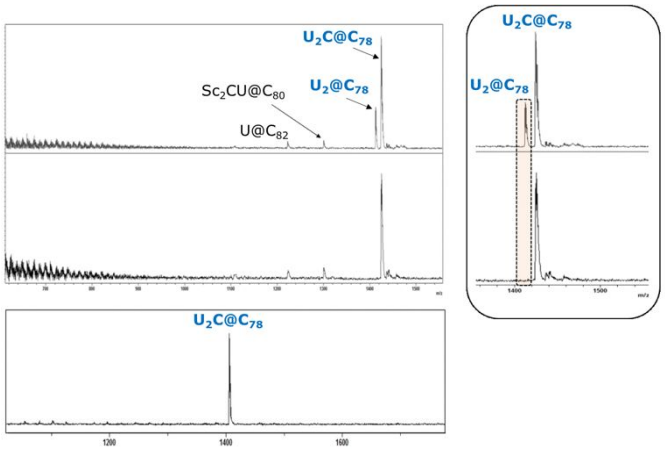

Figure 5. LDI-TOF monitoring the remaining supernatant over time during the selective molecular recognition of $U_2@C_{78}$ in front $U_2C@C_{78}$ (top); spectrum of pure $U_2@C_{78}$ released from **1**·$(BArF)_8$ (bottom).

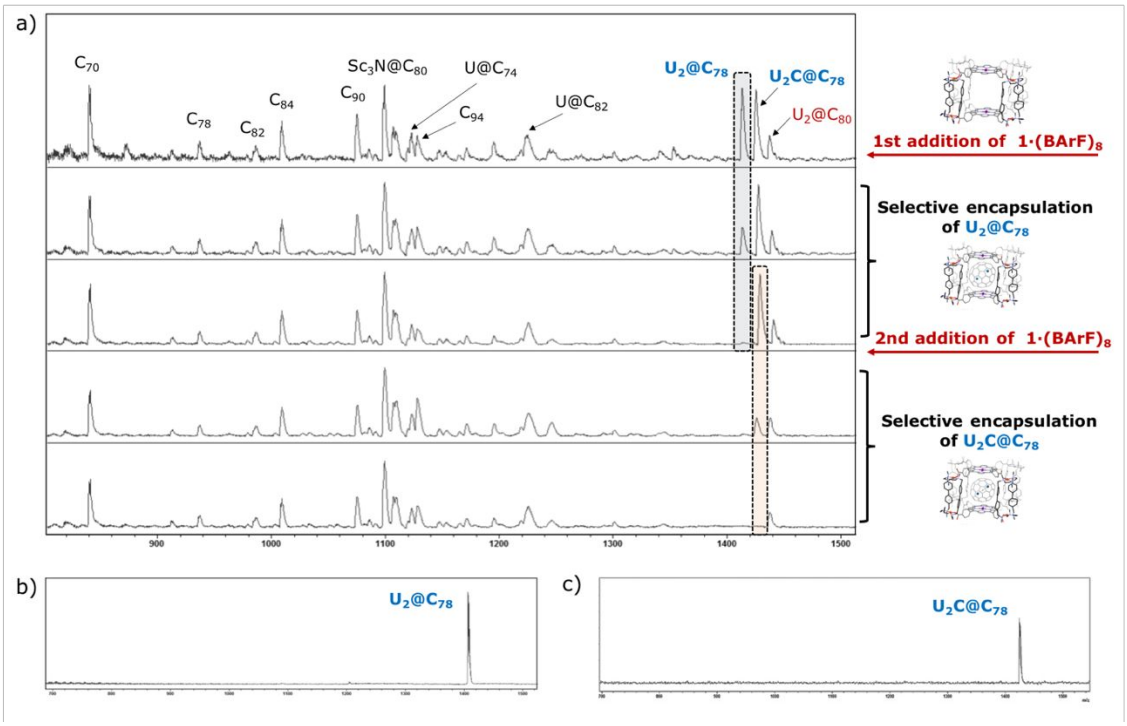

Figure 6. a) LDI-TOF monitoring the remaining supernatant over time during the selective molecular recognition of $U_2@C_{78}$; b) spectrum of pure $U_2@C_{78}$ and c) pure $U_2@C_{78}$ released from **1**·$(BArF)_8$.

ARTICLE

To gain a deeper understanding of the reasons behind the selectivity of **1**·(BArF)$_8$ for di-Uranium@C_{78} EMFs, DFT calculations were performed to compute the binding energies (BEs) between the two porphyrins of the nanocapsule and the EMFs U_2@I_h-C_{80} and U_2@D_{3h}-C_{78} in a similar manner as previously reported by us.[21] A systematic study has shown that the interaction energy between the porphyrins and the fullerenes changes significantly with the cage orientation with respect to the porphyrins. The position of the uranium ions inside these cages, however, does not affect so much the interaction energies. In particular, for the highly symmetric I_h-C_{80} the two U atoms have free rotation at room temperature. For D_{3h}-C_{78} the U atoms prefer to occupy the positions along the C_3 axis (Fig. 7 top).

The computed BEs between the EMF and the porphyrins for the structures represented in Fig. 7 are compiled in Table 1. These values from our simplified model would indicate that from a thermodynamic point of view the capture of the U_2@I_h-C_{80} EMF would be slightly favored, even though the relative binding energies and the porphyrin-porphyrin separations for the lowest energy orientations of the I_h-C_{80} and D_{3h}-C_{78} cages inside the nanocapsule are not that different. However, a more detailed inspection of the computed structures shows that the optimal dispositions of the EMFs display slightly shorter porphyrin – porphyrin separation for U_2@C_{78}. The difference is only about 0.2 Å, but it could be significant if we take into account that the empty nanocapsule **1**·(BArF)$_8$ used in the current experiments has a Zn···Zn separation of about 12 Å in the previously reported crystal structure,[21] considerably shorter than the equilibrium values computed in our models (Table 1).

To better evaluate the effect of the breathing of the cage, we have explored how the energy changes when the porphyrin-porphyrin distance shrinks from 14 Å to 13 Å. For the energy scan in Figure 8, the structures of the porphyrins and EMFs remain frozen and only the porphyrin-porphyrin distance changes. The values in Figure 8 and Table 2 confirm three main points: 1) the optimal Zn-Zn distances are somewhat longer for I_h-C_{80} EMFs, 2) the binding energy between porphyrin and EMF is slightly larger for I_h-C_{80} and 3) as the porphyrin-porphyrin compression progresses the binding energy increases with a lower slope for D_{3h}-C_{78}. Because of the cylindrical shape of D_{3h}-C_{78} cage, the energy destabilization of the system is smaller for this fullerene. Differences of BEs between structures **2** and **4** is larger than 8 kcal·mol^{-1} at a Zn-Zn distance of 13 Å, the D_{3h}-C_{78} EMF displaying the largest encapsulation energy. Interestingly, if we allow the fullerene to relax its structure, we observe that C_{80} reorients with respect to the porphyrins at 13 Å, and its BE increases from -33.6 to -38.8 kcal·mol^{-1}, whereas the reorganization for the D_{3h}-C_{78} cage is somewhat smaller with an energy change of 3.55 kcal·mol^{-1}, from -41.1 to -44.6 kcal·mol^{-1}. Thus, the binding energy difference between the two EMFs is still larger than 6 kcal·mol^{-1}. These results suggest that the shape of D_{3h}-C_{78} is more suitable than that of I_h-C_{80} for a relatively small nanocapsule like **1**·(BArF)$_8$, or similarly, that the energy penalty for the breathing of the nanocapsule to catch the EMF is smaller for the flattened D_{3h}-C_{78} than for the spherical I_h-C_{80}. This breathing ability is somewhat reminiscent of the one exhibited by some MOFs.[23]

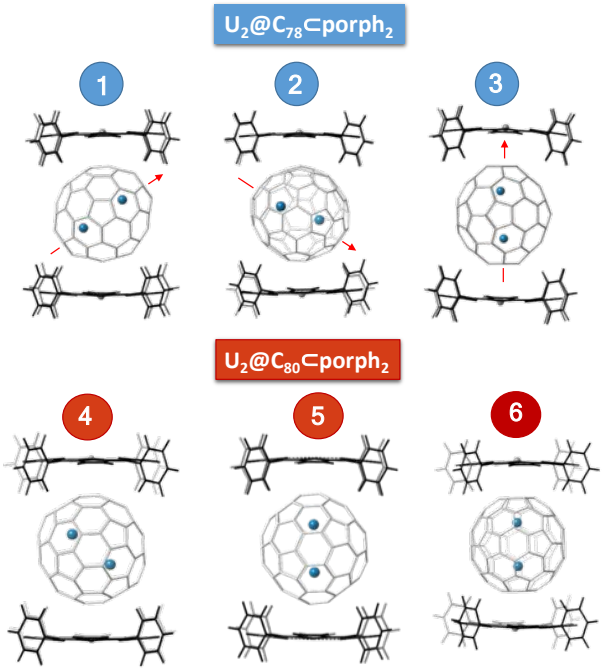

Figure 7. The lowest energy orientation of U_2@D_{3h}-C_{78} (top) and U_2@I_h-C_{80} (bottom) in a simplified two tetraphenyl-porphyrin model.

Table 1. Binding energies between the endohedral fullerene and two porphyrins.

	U_2@D_{3h}-C_{78}			U_2@I_h-C_{80}		
	1	**2**	**3**	**4**	**5**	**6**
BE [a]	-58.5	-56.9	-48.4	-59.1	-58.9	-52.4
d(Zn···Zn)[b]	13.68	13.65	14.48	13.80	13.95	14.26

a) Binding energies computed at the BLYP/TZP(D3) level are given in kcal·mol^{-1}; b) Zn···Zn separations are in Å.

A similar behavior was observed for U_2C@D_{3h}-C_{78}. When an extra C is added in the center of the U_2@C_{78} fullerene, affording a linear U_2C cluster as the most stable conformer, the porphyrin-porphyrin separation and the calculated binding energies are exactly the same as those found for U_2@D_{3h}-C_{78} (Figure S5). Although very recently DFT calculations for several U_2C@C_{2n} endofullerenes including U_2C@D_{3h}-C_{78} suggested that the U=C=U cluster takes a

bent form inside the D_{3h}-C_{78} cage,[24] we have verified that the linear arrangement is significantly lower in energy (Figure S6). The presence of the central carbon atom and the change in the formal oxidation state of uranium ions from +3 to +5 hardly modifies the electron density on the fullerene surface, as suggested by the molecular electrostatic potential distribution maps represented in Figure 9. Thus, our very simplified model cannot discriminate the different behavior observed for $U_2C@D_{3h}$-C_{78} and $U_2@D_{3h}$-C_{78} endohedral metallofullerenes, since the uranium carbide is only captured once $U_2@D_{3h}$-C_{78} has been completely removed from the soot (Fig. 5 and 6). This means that more sophisticated models and, probably, molecular dynamics simulations will be needed to better understand into the phenomena of encapsulation of fullerenes by nanocapsules like 1·$(BArF)_8$ or similar ones.

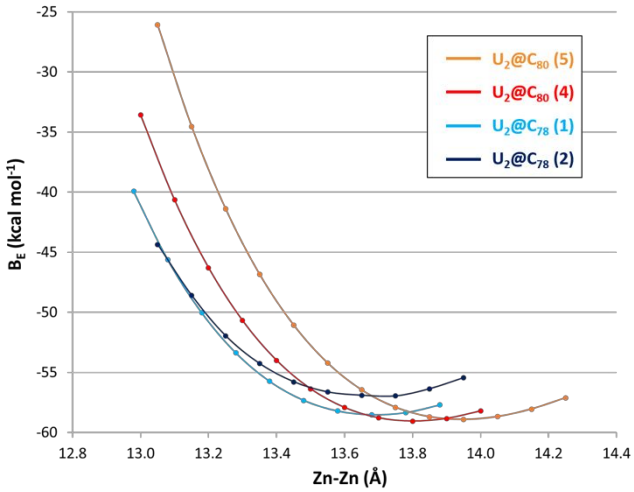

Figure 8. Energy scan along the Zn···Zn separation maintaining porphyrins and fullerenes fixed. The EMF numeration is identical to that in Figure 7.

Table 2. Binding energies[a] between the endohedral fullerene and two porphyrin model at different Porph···Porph distance.

	$U_2@D_{3h}$-C_{78}		$U_2@I_h$-C_{80}	
d(Zn···Zn)[b]	**1**	**2**	**4**	**5**
13.0	-41.1	-41.9	-33.7	-21.5
13.2	-50.6	-50.4	-46.3	-38.1
13.4	-56.0	-55.2	-54.1	-49.1
13.6	-58.2	-57.0	-58.0	-55.5
13.8	-58.1	-56.7	-59.1	-58.4
14.0	-56.6	-55.1	-58.3	-58.8

a) Binding energies computed at the BLYP/TZP(D3) level are given in kcal·mol^{-1}; b) Zn···Zn separations are in Å.

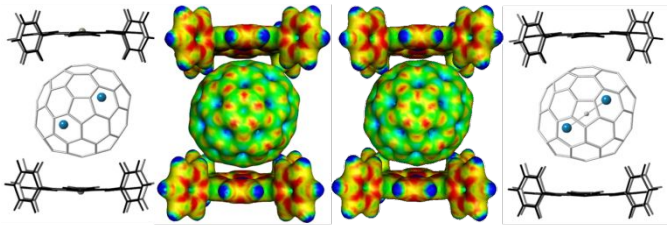

Figure 9. Comparison of computed structures and molecular electrostatic potential maps for $U_2@D_{3h}$-$C_{78} \subset porph_2$ (left, structure **1** in Figure 7) and $U_2C@D_{3h}$-$C_{78} \subset porph_2$ in their optimal orientations.

Conclusions

In summary, we report here the ability of supramolecular nanocapsule **1**·$(BArF)_8$ to selectively encapsulate U-based EMFs from highly complex soots containing empty fullerenes and EMFs, ranging from C_{60} to C_{96}. Moreover, the supramolecular host is capable discriminating C_{78}-based EMFs from C_{80}-based EMFs, thus showing an exquisite ability to discriminate among very similar EMFs. This selectivity stems from the shape differences between a spherical I_h-C_{80} and a flattened D_{3h}-C_{78} carbon cage, which induce an enhanced interaction between the carbon cage and the porphyrin units of the host. Computational analysis also suggests that the breathing ability of the host in the solid state is somewhat limited and that results in a lower breathing energy penalty towards a highly favourable encapsulation of the flattened D_{3h}-C_{78}-based EMF. Moreover, nanocapsule **1**·$(BArF)_8$ can also sequentially and selectively encapsulate the same D_{3h}-C_{78} carbon cage differing only in the nature of the endohedral cluster, i.e U_2 vs U_2C. This indicates that besides the shape of the carbon cage, the cluster electronics are at interplay in finally determining the affinity for the host. The non-chromatographic supramolecular purification of U-based EMFs reported here has proven to be a viable alternative to HPLC methods, and pure $U_2@D_{3h}$-C_{78} and $U_2C@D_{3h}$-C_{78} EMFs may be accumulated and potentially find utility in several research fields. Moreover, nanocapsule **1**·$(BArF)_8$ and other supramolecular analogues might be designed as platforms to selectively purify targeted EMFs of interest in complex soots.

Conflicts of interest

There are no conflicts to declare.

Acknowledgements

We acknowledge financial support from GenCat (2017 SGR 264 and 2017 SGR 629) and MINECO-Spain (CTQ2016-77989-P and CTQ2017-87269-P). L.E. thanks the US National Science Foundation (NSF) for generous support of this work under the NSF-PREM program (DMR-1205302) and CHE-1408865. The Robert A. Welch Foundation is also gratefully acknowledged for

an endowed chair to LE (Grant AH-0033). X.R. and J.M.P. are also grateful to ICREA foundation for ICREA-Acadèmia awards.

Notes and references

1. S. Yang, T. Wei and F. Jin, *Chem. Soc. Rev.*, 2017, **46**, 5005-5058.
2. X. Lu, T. Akasaka and S. Nagase, *Chem. Commun.*, 2011, **47**, 5942-5957.
3. X. Zhang, Y. Wang, R. Morales-Martínez, J. Zhong, C. de Graaf, A. Rodríguez-Fortea, J. M. Poblet, L. Echegoyen, L. Feng and N. Chen, *J. Am. Chem. Soc.*, 2018, **140**, 3907-3915.
4. X. Zhang, W. Li, L. Feng, X. Chen, A. Hansen, S. Grimme, S. Fortier, D.-C. Sergentu, T. J. Duignan, J. Autschbach, S. Wang, Y. Wang, G. Velkos, A. A. Popov, N. Aghdassi, S. TDuhm, X. Li, J. Li, L. Echegoyen, W. H. E. Schwarz and N. Chen, *Nat. Comm.*, 2018, **9**, 2753.
5. R. Westerström, J. Dreiser, C. Piamonteze, M. Muntwiler, S. Weyeneth, H. Brune, S. Rusponi, F. Nolting, A. Popov, S. Yang, L. Dunsch and T. Greber, *J. Am. Chem. Soc.*, 2012, **134**, 9840-9843.
6. S. Osuna, M. Swart and M. Solà, *J. Am. Chem. Soc.*, 2009, **131**, 129-139.
7. S. Osuna, M. Swart, J. M. Campanera, J. M. Poblet and M. Solà, *J. Am. Chem. Soc.*, 2008, **130**, 6206-6214.
8. M. Garcia-Borràs, S. Osuna, J. M. Luis, M. Swart and M. Solà, *Chem. Eur. J.*, 2012, **18**, 7141-7154.
9. N. Martín, *Chem. Commun.*, 2006, DOI: 10.1039/B601582B, 2093-2104.
10. C. M. Cardona, A. Kitaygorodskiy and L. Echegoyen, *J. Am. Chem. Soc.*, 2005, **127**, 10448-10453.
11. Y. Iiduka, O. Ikenaga, A. Sakuraba, T. Wakahara, T. Tsuchiya, Y. Maeda, T. Nakahodo, T. Akasaka, M. Kako, N. Mizorogi and S. Nagase, *J. Am. Chem. Soc.*, 2005, **127**, 9956-9957.
12. H. Shinohara and N. Tagmatarchis, in *Endohedral Metallofullerenes*, Wiley, 2015, DOI: 10.1002/9781118698006.ch4, pp. 43-68.
13. S. Stevenson, K. Harich, H. Yu, R. R. Stephen, D. Heaps, C. Coumbe and J. P. Phillips, *J. Am. Chem. Soc.*, 2006, **128**, 8829-8835.
14. S. Stevenson, M. A. Mackey, J. E. Pickens, M. A. Stuart, B. S. Confait and J. P. Phillips, *Inorg. Chem.*, 2009, **48**, 11685-11690.
15. K. Akiyama, T. Hamano, Y. Nakanishi, E. Takeuchi, S. Noda, Z. Wang, S. Kubuki and H. Shinohara, *J. Am. Chem. Soc.*, 2012, **134**, 9762-9767.
16. M. R. Cerón, F. F. Li and L. Echegoyen, *Chem. Eur. J.*, 2013, **19**, 7410-7415.
17. L. P. Hernández-Eguía, E. C. Escudero-Adán, J. R. Pinzón, L. Echegoyen and P. Ballester, *J. Org. Chem.*, 2011, **76**, 3258-3265.
18. M.-Y. Ku, S.-J. Huang, S.-L. Huang, Y.-H. Liu, C.-C. Lai, S.-M. Peng and S.-H. Chiu, *Chem. Commun.*, 2014, **50**, 11709-11712.
19. Y. Nakanishi, H. Omachi, S. Matsuura, Y. Miyata, R. Kitaura, Y. Segawa, K. Itami and H. Shinohara, *Angew. Chem. Int. Ed.*, 2014, **53**, 3102-3106.
20. C. Fuertes-Espinosa, C. García-Simón, E. Castro, M. Costas, L. Echegoyen and X. Ribas, *Chem. Eur. J.*, 2017, **23**, 3553-3557.
21. C. Fuertes-Espinosa, A. Gómez-Torres, R. Morales-Martínez, A. Rodríguez-Fortea, C. García-Simón, F. Gándara, I. Imaz, J. Juanhuix, D. Maspoch, J. M. Poblet, L. Echegoyen and X. Ribas, *Angew. Chem. Int. Ed.*, 2018, **57**, 11294-11299.
22. C. García-Simón, M. Garcia-Borràs, L. Gómez, T. Parella, S. Osuna, J. Juanhuix, I. Imaz, D. Maspoch, M. Costas and X. Ribas, *Nat. Commun.*, 2014, **5**, 5557.
23. A. Schneemann, V. Bon, I. Schwedler, I. Senkovska, S. Kaskel and R. A. Fischer, *Chem. Soc. Rev.*, 2014, **43**, 6062-6096.
24. Y. Li, L. Yang, Z. Li, Q. Hou, L. Li and P. Jin, *Inorg. Chem.*, 2019, **58**, 10648-10655.

TOC text

A supramolecular nanocapsule can effectively separate C_{78}-based over C_{80}-based EMFs based on the shape preference for flattened C_{78}-based EMFs.

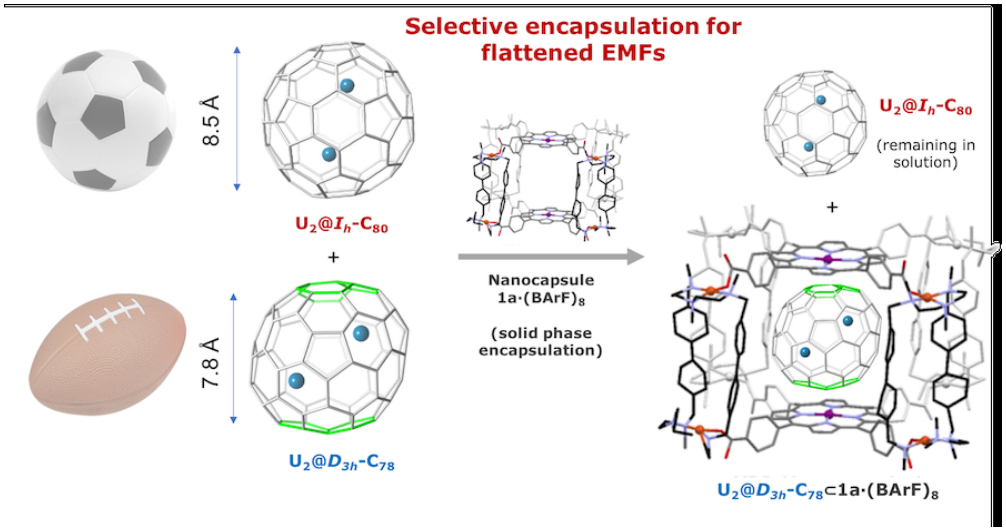
Selective encapsulation for flattened EMFs
8.5 Å
U2@Ih-C80
+
7.8 Å
U2@D3h-C78
Nanocapsule 1a·(BArF)8
(solid phase encapsulation)
U2@Ih-C80
(remaining in solution)
+
U2@D3h-C78⊂1a·(BArF)8